Chemistry–A European Journal
Research Article
doi.org/10.1002/chem.202402382
Chemistry Europe
European Chemical Societies Publishing
www.chemeurj.org

Transient Photoactivation of Anionophores by Using Redshifted Fast-Relaxing Azobenzenes

Aidan Kerckhoffs,[a] Manzoor Ahmad,[a] and Matthew J. Langton*[a]

Photo-regulated transmembrane ionophores enable spatial and temporal control over activity, offering promise as targeted therapeutics. Key to such applications is control using biocompatible visible light. Herein, we report red-shifted azobenzene-derived synthetic anionophores that use amber or red light to trigger (*E*)-(*Z*) photoisomerisation and activation of transmembrane chloride transport. We demonstrate that by tuning the thermal half-life of the more active, but thermodynamically unstable, Z isomer to relax on the timescale of minutes, transient activation of ion transport can be achieved by activating solely with visible light and deactivating by thermal relaxation.

Introduction

The precise regulation of ion transport across cell membranes is crucial to many biological processes[1] and is controlled by membrane proteins, which are themselves regulated by external stimuli such as small-molecules, membrane potential and light.[2] Synthetic small-molecule ionophores have experienced a burgeoning interest over the last 10–20 years;[3–5] showing promise as novel therapeutics for channelopathies (diseases arising from faulty ion channels) such as cystic fibrosis,[6] and for triggering apoptotic pathways in cancer cells.[7] However, disrupting ionic gradients in off-target cells may lead to severe side-effects in a therapeutic context.[8] This has spurred the development of stimuli-responsive ion carriers,[9] enabling targeted control of ion transport using external stimuli including light,[10–13] voltage,[14] enzymes[15,16] or redox.[17,18] Amongst these stimuli, light is arguably one of the most attractive for manipulating biological systems due to its high spatiotemporal precision, non-invasive nature and wavelength-dependent orthogonality.[19] In the field of photo-pharmacology, incorporation of light-responsive moieties into drugs allows for irreversible or reversible modulation of their activity,[20] where appropriately timed photo-isomerisation may be used to fine-tune the behaviour of the drug to maximise its therapeutic window.[21] For example, if the active (e.g. (*Z*)-isomer) and inactive (e.g. (*E*)-isomer) forms of the drug exhibit differing permeabilities and absorption properties, precise timing of when the drug is activated and deactivated enables control of blood plasma concentrations.[22] Azobenzenes (ABs) are attractive photoswitches in this regard due to their robust switching and large conformational changes upon isomerisation,[23] and have found numerous applications within photopharmacology, such as to generate photoswitchable antibiotics,[24,25] glutamate receptor agonists[26] and other switchable drugs spanning over 100 biological targets.[27,28]

Within the field of synthetic ion transporters, the vast majority of light-regulated systems are activated by UV light.[9,12,29] However, UV light can damage cellular surroundings and exhibits low tissue penetration, limiting its use *in vivo*.[30] This has spurred the development of photoswitches that respond to higher wavelengths (lower energies) of light.[23,31,32] Recently, we reported photoswitchable 'on/off' transporters **F_4-sq** and **Cl_4-sq** that are switched 'on' using green[33] or red light,[34] by isomerisation of a bis-squaramide-appended azobenzene from the (*E*) to (*Z*) isomer (Figure 1). However, due to the long thermal half-life of the (*Z*)-isomer in both systems, ion transport could only be switched 'off' by irradiation with blue light to form a photostationary state (PSS) containing ~85% of the (*E*)-isomer. To the best of our knowledge, there are no 'on/off' transporters that exclusively use deeply redshifted wavelengths of light, presumably because both isomers of a photoswitch require unique and orthogonal absorption profiles to reversibly isomerise to a significant degree.[35] One method of overcoming this limitation of molecular photoswitches is to employ a fast-relaxing (~seconds to minutes) thermodynamically unstable isomer of the switch as the transport-active species, thus allowing significant accumulation of the metastable 'on' state under photo-irradiation, but with sufficiently rapid thermal relaxation to re-form the 'off' state.[36] Herein, we demonstrate this concept and report the first examples of synthetic ion transporters capable of spatiotemporally controlling ion flux using only thermal relaxation and biocompatible wavelengths of light.

[a] *A. Kerckhoffs, M. Ahmad, M. J. Langton*
Department of Chemistry, Chemistry Research Laboratory, University of Oxford, Mansfield Road, Oxford OX1 3TA, UK
E-mail: matthew.langton@chem.ox.ac.uk

Supporting information for this article is available on the WWW under https://doi.org/10.1002/chem.202402382

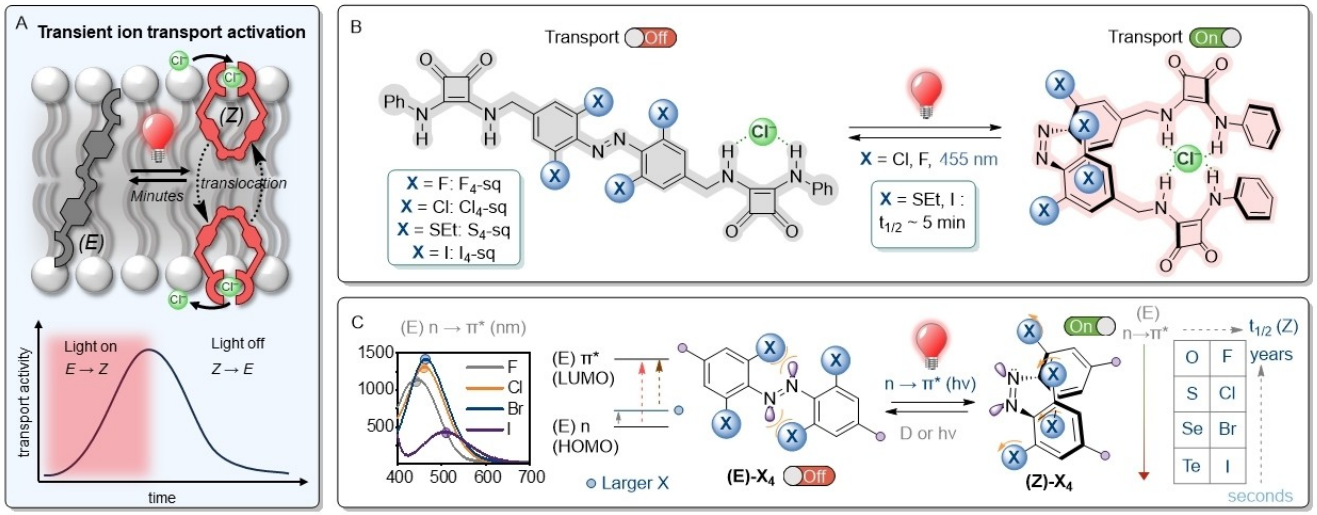

Figure 1. (A) Schematic representation of transient anionophore activation by one-colour photoswitching and thermal relaxation. (B) Structures of fast relaxing photoswitchable transporters **S_4-sq** and **I_4-sq** studied in this work, and previously reported two-colour 'on/off' photoswitchable ion transporters **F_4-sq** and **Cl_4-sq**. (C) Periodic trends of the family of tetra-*ortho*-azobenzenes, from which the systems used here are derived, where heavier tetra-*ortho* chalcogen and halogen atoms red-shift the (*E*) n→π* transitions and shorten the (*Z*) thermal half-lives. UV-Vis data is for the CH_2NHBoc derivative.[37]

Results and Discussion

Approach

The groups of Hecht and Woolley have pioneered the development of red-shifted azobenzene derivatives, through tetra-*ortho*-substitution with lighter chalcogen[37] and halogen[31,38] heteroatoms. Recently, we extended the series to include derivatives substituted with all accessible group 16 and 17 elements, and demonstrated that larger, less electronegative chalcogen and halogen *ortho* substituents redshift the (*E*) n→π* transition (and hence the wavelength at which isomerisation can be triggered), whilst also reducing the (*Z*)-isomer half-life (Figure 1C).[39] This can be rationalised by larger *ortho* substituents in the (*E*) isomer experiencing more repulsive interactions between the diazo lone pairs, leading to destabilisation of the n molecular orbital and a red-shifting in the average n→π* transitions.[39] Conversely, electronegative substituents relieve the (*Z*) isomer N=N lone pair repulsion and stabilise the overall Z isomer energy, leading to longer half-lives.

The tetra *ortho* thio and iodo derivatives display (*Z*)-isomer thermal half-lives in the order of ~5 min, and the (*E*)-isomers of both respond to red wavelengths of light generating a PSS with ~50% (*Z*), and demonstrating that photoisomerization is not outcompeted by the relatively fast thermal relaxation process when irradiated with LEDs (Figure S18). We identified the (*Z*)-isomers of these derivatives as possessing suitable thermal half-lives for the development of a transiently active ionophores, accessible by replacing the F and Cl *ortho* substituents of our previously reported switchable anionophores **F_4-sq** and **Cl_4-sq** with sulfur or iodine atoms to afford **S_4-sq** and **I_4-sq** (Figure 1B). In these systems, the (*E*)-isomer binds and transports chloride weakly. Upon isomerisation with biocompatible red light to the more compact (*Z*)-isomer, cooperativity between anion receptors, greater degrees of anion encapsulation[40] and increased mobility relative to the large, extended (*E*)-isomer[41] results in greater transport rates (Figure 1B). By using an unstable photoswitch that relaxes from the (*Z*)-isomer back to the inactive (*E*)-isomer at a suitable rate, we anticipated that precisely timed 'on/off' switching of transmembrane ion transport controlled using light and thermal relaxation would be achievable. In our previous studies,[33,34] the phenyl squaramide unit was found to be the optimal substituent for achieving excellent 'on/off' behaviour.

Synthesis and Photoswitching Properties

Fast relaxing squaramide transporters **S_4-sq** and **I_4-sq** were prepared from the corresponding Boc-protected amino-derivatives **S_4-NHBoc** and **I_4-NHBoc** (Figure 2A).[39] To confirm the fast-relaxing nature of these species, we determined the thermal half-life in DMSO after irradiation with either amber (590 nm, 300 mW) or red (625 nm, 920 mW) LEDs. The (*Z*)-isomer thermal

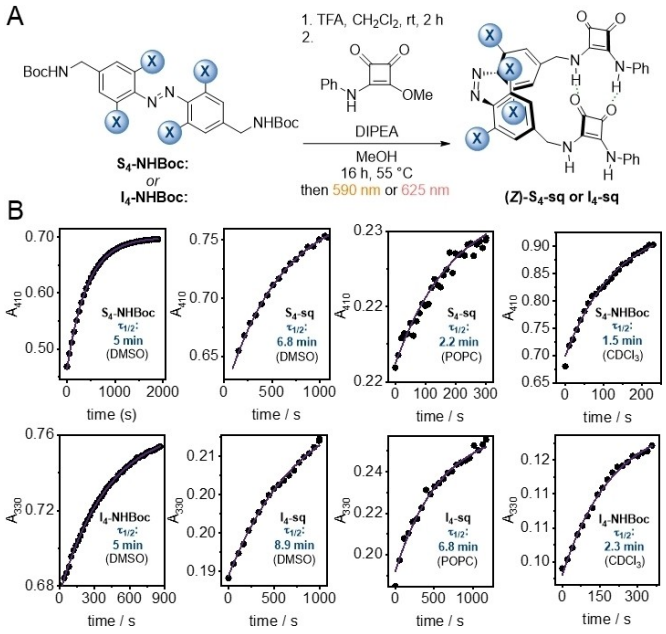

Figure 2. (A) Synthesis of fast-relaxing ionophores **S_4-sq** and **I_4-sq**. (B) Thermal half-lives in solvent (~50 μM) and POPC lipid vesicles (2.5 mM lipids; 1 mol% X_4-sq relative to lipids).

half-life increased from 5 to ~7 min for **S_4-sq** and from 5 to 9 min for **I_4-sq**, when compared to the Boc-protected precursor. This may be attributed to intramolecular hydrogen bonding between the two squaramide motifs in the (*Z*)-isomers stabilising the species. These observations are in-line with our reports for other (*Z*)-**I_4** derivatives, where photoswitches appended with derivatives capable of forming intramolecular hydrogen bonds (e.g. NHBoc) exhibit longer half-lives than those without (e.g. N-phthalimide).[39] Moreover, in a similar azobenzene-derived photoswitchable anion receptor system, we have demonstrated that upon reversible chloride binding there is a significant increase in (*Z*)-isomer thermal half-life relative to the unbound form, which is attributed to overall stabilisation of the (*Z*)-Cl^- complex.[42]

When the compounds were embedded within 200 nm 1-palmitoyl-2-oleoyl-glycero-3-phosphocholine (POPC) vesicles buffered to pH 7.0 in NaCl solution (the conditions that subsequent ion transport experiments were conducted), the thermal half-life decreased to ~2 min for **S_4-sq** and ~7 min **I_4-sq**. This decrease may be tentatively attributed to the lower polarity environment favouring a non-polar transition state during isomerisation, leading to a shorter thermal half-life; typical for *ortho*-halogenated ABs. Indeed, the half-life of **S_4-NHBoc** in the less polar $CDCl_3$ is lowered to 1.5 min (relative to 5 min in more polar DMSO). The half-life of **I_4-sq** decreased to 2.3 min in $CDCl_3$.

Anion Transport Studies

The anion transport activities of both derivatives were studied in phosphocholine large unilamellar vesicles (POPC LUVs, lipid concentration 31 μM), loaded with 8-hydroxypyrene-1,3,6-trisulfonate (HPTS) buffered to pH 7.0 in NaCl solution. HPTS is a pH-sensitive fluorophore with a pK_a~7.3: the protonated and deprotonated forms exhibit unique fluorescence excitation spectra, which enables ratiometric analysis of the internal pH of the LUVs during the transport assay. A pH gradient was applied across the membrane by addition of a base pulse, followed by addition of the carrier as a DMSO solution (< 0.5% v/v). The ability of the anionophore to dissipate the pH gradient by transmembrane ion transport was determined by recording the change in the HPTS emission, I_{rel} (λ_{em} = 510 nm), with time following excitation at λ_{ex} = 405/465 nm (Figure 3A, B, E and F). Detergent (Triton X-100) was added at the end of each experiment to lyse the vesicles for calibration. For the (*Z*) isomers, the experiment was run by pre-irradiating the samples with 590 nm light (**S_4-sq**) or red 625 nm light (**I_4-sq**) for 5 min. Previous studies have shown that such squaramide appended azobenzenes operate as a H^+/Cl^- symporter or Cl^-/OH^- antiporter anion carrier.[33]

The concentration dependence of the activity of the (*E*) and (*Z*) isomers of each anion carrier was determined by adding increasing concentrations of the transporter in DMSO. The fractional activities (relative intensity just prior to lysis) were plotted as a function of concentration and the dose–response curves fitted to the Hill equation. This is used to describe the dependence of the anion transport activity (reported by I_{rel}) on the *n*-th power of the carrier concentration, and facilitates comparison of the relative activities of carriers through an effective concentration value (EC_{50}) required to reach 50% activity (see ESI section 4 for full transport data).

In the case of **S_4-sq**, the enhancement in EC_{50} between the (*E*) and (*Z*)-isomers was 2-fold (Figure 3C). The less pronounced increase in transport rates for **S_4-sq** relative to the analogous halogen compounds **F_4-sq** and **Cl_4-sq** (~8-fold)[33] may in-part be due to the ethyl groups in (*E*)-**S_4-sq** disrupting dimerisation or oligomerisation within the membrane, leading to faster transport rates (EC_{50} = 32 nM, compared to 180 nM for *(E)*-**Cl_4-sq**). Previously, we have shown that dimerization to inactive species in *(E)*-**Cl_4-sq** is a key effect towards suppressing the activity of the (*E*) isomer, and improving transport enhancements upon isomerisation.[33] Indeed, *(Z)*-**Cl_4-sq** (EC_{50}~22 nM) is comparable to that of (*Z*)-**S_4-sq**, where dimerization effects are expected to no longer take place. Furthermore, given the relatively fast thermal relaxation of (*Z*)-**S_4-sq** ($t_{1/2}$ = 2.2 min), significant relaxation back to the less active (*E*) isomer will occur during the timescale of the assay. Therefore, this Hill analysis, which analyses the fractional activity at 290 s at the end of the assay immediately prior to lysis, provides an underestimation of (*Z*)-isomer activity. To mitigate the effects of thermal isomerisation in the analysis, the initial rates of transport were determined for each concentration (Figures 3D and S25–S29). Both isomers displayed sigmoidal dose-response behaviours, with around 6-fold enhancement in transport rates observed at the higher loadings, and a 4-fold enhancement at 250 nM (ESI Figure S27). This demonstrates that the activity of the anionophore decreases over the ~3 min duration of the experiment,

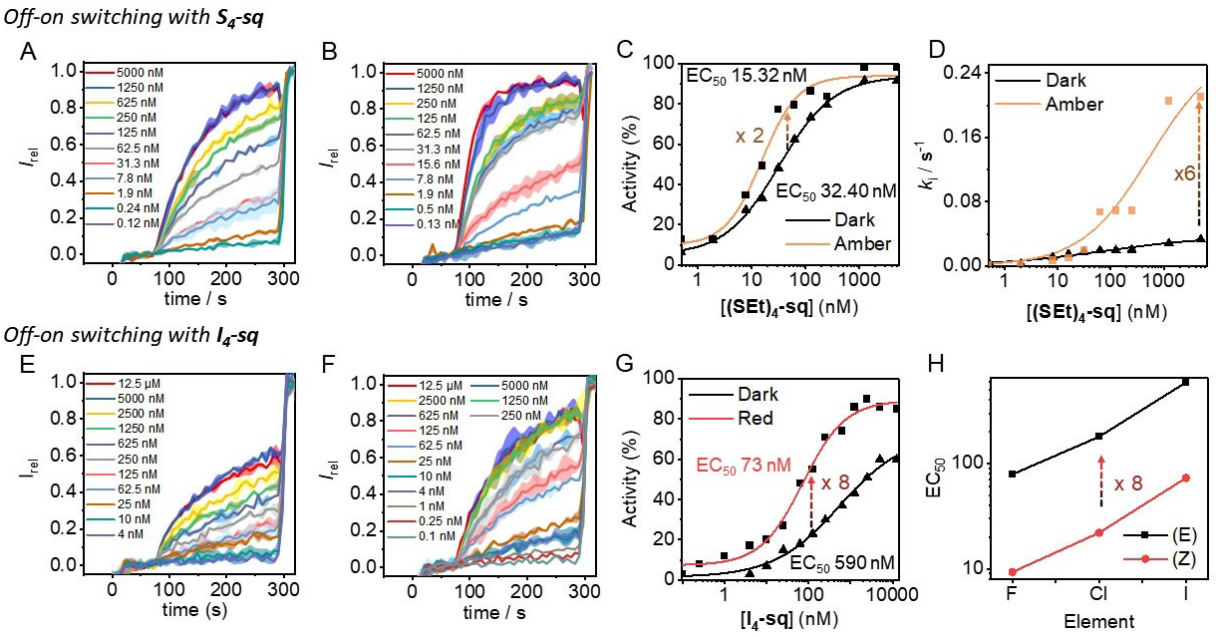

Figure 3. (A) Transport data for (*E*)-**S_4-sq** and (B) (*Z*)-**S_4-sq** using HPTS assay. (C) Dependence on I_{rel} immediately prior to lysis on concentration of (*E*)-**S_4-sq** (▲) and (*Z*)-**S_4-sq** (■); fit to the Hill equation (solid line). (D) Dependence of initial rates of anion transport for **S_4-sq** on ionophore concentration; fit to the Hill equation (solid line). (E) Transport Data for (*E*)-**I_4-sq** and (F) (*Z*)-**I_4-sq** using the HPTS assay. (G) Dependence on I_{rel} immediately prior to lysis on concentration of (*E*)-**I_4-sq** (▲) and **(*Z*)-I_4-sq** (■); fit to the Hill equation (solid line). (H) Dependence of halogen substituent on EC_{50} enhancements in HPTS assay

consistent with the (*Z*) to (*E*) thermal half-life of ~2 min in POPC vesicles.

The analogous transport experiments were then conducted for **I_4-sq**, which exhibits a longer thermal half-life for (*Z*) to (*E*) isomerisation of 6.8 min in POPC vesicles. The enhancement in EC_{50} was significantly increased upon isomerisation (8-fold, Figure 3G), displaying similar behaviour to the metastable **F_4-sq** and **Cl_4-sq** counterparts. Interestingly, across the homologous series of halogenated **X_4-sq** derivatives, the EC_{50} enhancement between the (*E*) and (Z) isomers is consistently around ~8-fold, with absolute EC_{50} values increasing with larger atomic weights (Figure 3H). This may be due to decreased mobility with increasing molecular weight, or the increase in lipophilicity with increasing halogen size hampering the transport efficiency of each derivative.[43] Indeed, it has been previously shown that within a series of structurally similar anion transporters, there appears to be an optimal log P value, typically around 4–5,[44,45] reflecting a balance between membrane deliverability and mobility within the bilayer. Indeed, **F_4-sq** displays a clogP value of ~4.8,[33] whereas for **Cl_4-sq** and **I_4-sq**, these values are 7.1 and 8.7, respectively.

Given the observed reduction in activity of **S_4-sq** over the timescale of the transport experiment due to the relatively fast thermal relaxation kinetics of (*Z*)-**S_4-sq** ($t_{1/2}$ = 2.2 min in POPC vesicles), we sought to further explore this phenomenon using *in-situ* constant irradiation conditions, whereby the transport activity is determined whilst the sample is continually irradiated with an LED. To this end, the HPTS anion transport assay was rerun at the EC_{50} of the (*E*) isomer (32 nM; 0.1 mol% relative to lipid). The experiment was conducted with *in-situ* irradiation of the cuvette within the spectrometer using a 590 nm LED (300 mW), with a 510 nm band pass filter in front of the detector to allow for detection of the HPTS emission without interference from the incident light from the LED and prevent damage to the detector (see ESI for further details). Pleasingly, irradiation of the vesicles containing (*E*)-**S_4-sq** with 590 nm light to isomerise to (*Z*)-**S_4-sq** resulted in detectable increase in transport rates (Figure 4A), whilst when the light was switched off, the transport rate decreased. These results are consistent with those from *ex-situ* isomerisation experiments (Figure 3C and D), which also revealed the reduction in relative activity of the Z isomer over the course of the assay in the absence of irradiation. However, poor signal to noise due to the presence

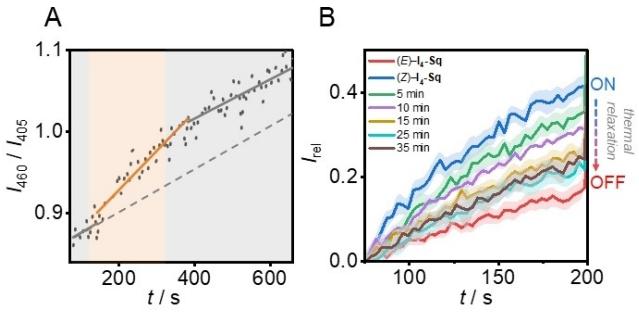

Figure 4. (A) Modulation of ion transport rates using S_4-sq (0.1 mol % wrt. lipids) by *in-situ*, real-time irradiation of vesicles with 590 nm light (orange shading) and allowing thermal relaxation to take place (dark, grey shading). Dashed grey line: extrapolation of dark-state transport kinetics, to guide the eye. (B) Modulation of ion transport rates by pre-irradiating vesicles containing I_4-sq with 625 nm light and allowing varying time delays before initiation of ion transport (HPTS assay, 0.2 mol% with respect to lipid).

of the band pass filter in front of the detector prevented a more detailed analysis using this experimental set-up.

The longer-lived iodo-derivative (*Z*)-**I_4-sq** isomer was more amenable to the *in-situ*, direct quantification of the time dependence of transport rates, because the time-scale of the thermal relaxation determined in POPC vesicles was longer than the transport experiment ($t_{1/2}$ = 6.8 min), and so constant irradiation whilst simultaneously measuring the HPTS emission was not required. Accordingly, to elucidate the ability of the longer-lived (*Z*)-**I_4-sq** to modulate the anion transport rate, (*E*)-**I_4-sq** was pre-incorporated within POPC vesicles containing HPTS. The vesicles were then subjected to irradiation with red light (625 nm) to generate (*Z*)-**I_4-sq**, and the transport activity recorded by addition of a base pulse to initiate chloride transport (Figure 4B). The activity was also recorded on separate samples after varying time delays following irradiation, to allow for thermal relaxation to (*E*)-**I_4-sq**. As anticipated from the previously determined $t_{1/2}$ value of ~7 min, the transport rates decreased with increasing time delays with a comparable half-life (reaching approximately 50% activity after 10 min, compared to the (*Z*)-isomer rich PSS). Together, these results demonstrate that by incorporating fast-relaxing photoswitches into photo-responsive ion transporters, off-on-off switching can be achieved using solely amber/red light and thermal relaxation of the ionophore.

Conclusions

We have demonstrated the first examples of temporal control of ion flux with synthetic transporters using only thermal relaxation and biocompatible wavelengths of light. By employing switchable anionophores in which the more active isomer is thermally unstable, pulsed ion transport activity could be achieved by using amber/red light to generate the active ionophore, and exploiting thermal relaxation to relax back to an off-state over time. The thermal relaxation half-life of these transporter systems could be tuned by varying the *ortho*-substituent of the azobenzene photoswitch. We anticipate that these results may provide insights into new ways to access transiently activated therapeutic ionophores, in which the activity and lifetime can be carefully controlled with spatiotemporal precision by pulsed irradiation of the target region.

Experimental Section

General experimental: All reagents and solvents were purchased from commercial sources and used without further purification. Lipids were purchased from Avanti Polar Lipids and used without further purification. Where necessary, solvents were dried by passing through an MBraun MPSP-800 column and degassed with nitrogen. Triethylamine was distilled from and stored over potassium hydroxide. Column chromatography was carried out on Merck® silica gel 60 under a positive pressure of nitrogen. Where mixtures of solvents were used, ratios are reported by volume. NMR spectra were recorded on a Bruker AVIII 400, Bruker AVII 500 (with cryoprobe) and Bruker AVIII 500 spectrometers. Chemical shifts are reported as δ values in ppm. Mass spectra were carried out on a Waters Micromass LCT and Bruker microTOF spectrometers. Fluorescence spectroscopic data were recorded using a Horiba Duetta fluorescence spectrophotometer, equipped with Peltier temperature controller and stirrer. UV-Vis spectra were recorded on a V-770 UV-Visible/NIR Spectrophotometer equipped with Peltier temperature controller and stirrer using quartz cuvettes of 1 cm path length. Experiments were conducted at 25 °C unless otherwise stated. Vesicles were prepared as described below using Avestin "LiposoFast" extruder apparatus, equipped with polycarbonate membranes with 200 nm pores. GPC purification of vesicles was carried out using GE Healthcare PD-10 desalting columns pre-packed with Sephadex G 25 medium.

Synthesis of S_4-Sq. To a solution of **S_4-NHBoc**[37] (70.0 mg, 103 μmol) in CH_2Cl_2 (1.50 mL) was added TFA (180 μL). The reaction was stirred at room temperature for 2 h. The TFA was removed under a stream of nitrogen, then dried in vacuo to afford the title compound as an orange solid (73.0 mg, 103 μmol, 100%) (*E*)-**S_4-NH_2**: 1H NMR (400 MHz, MeOD) δ 7.32 (s, 4H), 4.19 (s, 4H), 2.98 (q, J = 7.4 Hz, 8H), 1.32 (t, J = 7.4 Hz, 12H). ^{13}C NMR (126 MHz, MeOD) δ 148.08, 138.88, 135.79, 123.87, 44.05, 27.64, 13.78. HRMS-EI (m/z) Calculated for $C_{22}H_{33}N_4S_4$ $[M+H]^+$, 481.1583; found 481.1578. **S_4-NH_2** (39.0 mg, 55.0 μmol) was dissolved in MeOH (1.00 mL). DIPEA (580 μL, 0.330 mmol, 6 eq) was added dropwise. 3-methoxy-4-(phenylamino)cyclobut-3-ene-1,2-dione (22.4 mg, 110 μmol, 2 eq) in MeCN (1 mL) was added, and the solution was heated at 55 °C for 16 h. The reaction was cooled to rt and the solid precipitate was filtered and washed sequentially with MeOH and MeCN, then collected and dried under high vacuum to afford the title compound as an orange solid (30.0 mg, 36.5 μmol, 66%). *E*-S_4-sq: ^{1}H NMR (500 MHz, DMSO) δ 9.75 (s, 2H), 8.12 (s, 2H), 7.43 (d, *J* = 8.0 Hz, 4H), 7.37–7.32 (m, 4H), 7.27 (s, 4H), 7.04 (tt, *J* = 7.3, 1.2 Hz, 2H), 4.84 (s, 4H), 2.91 (q, *J* = 7.4 Hz, 8H), 1.20 (t, *J* = 7.3 Hz, 12H). ^{13}C NMR (126 MHz, DMSO) δ 184.51, 180.60, 168.90, 164.25, 145.13, 140.42, 138.88, 136.27, 129.36, 122.82, 121.34, 118.20, 46.96, 25.66, 13.35. HRMS-EI (m/z) Calculated for $C_{42}H_{41}O_4N_6S_4$ $[M+H]^+$, 821.2078; found 821.2072

Synthesis of I_4-Sq. To a solution of I_4-NHBoc[37] (32.0 mg, 34.0 μmol) in CH_2Cl_2 (2.00 mL) was added TFA (0.20 mL). The reaction was stirred at rt for 2 h. The TFA and solvent were removed by evaporation under a stream of nitrogen and then under high vacuum. The crude diamine was dissolved in MeOH (0.5 mL). DIPEA (30.0 μL) was added dropwise. 3-methoxy-4-(phenylamino)cyclobut-3-ene-1,2-dione (13.8 mg, 68.0 μmol, 2.00 eq) in MeCN (0.500 mL) was added, and the solution was heated at 40 °C for 16 h. The reaction was cooled to rt and the solid precipitate was filtered and washed sequentially with MeOH and MeCN, then collected and dried under high vacuum to afford the title compound as a purple solid (6.04 mg, 4.80 μmol, 14%). (*E*)-S_4-sq: ^{1}H NMR (600 MHz, DMSO) δ 9.75 (s, 2H, 8.12 (d, J = 5.8 Hz, 4H), 8.09–8.01 (m, 2H), 7.43 (d, J = 7.9 Hz, 4H), 7.37–7.32 (m, 4H), 7.04 (tt, J = 7.3, 1.2 Hz, 2H), 4.82 (d, J = 5.2 Hz, 4H). ^{13}C NMR (151 MHz, DMSO) δ 184.01, 180.68, 168.65, 164.15, 149.43, 143.07, 139.77, 138.85, 129.29, 122.77, 118.21, 91.25, 45.21. HRMS-EI (m/z) Calculated for $C_{34}H_{23}N_6O_4I_4$ $[M+H]^+$, 1086.7954; found 1086.7954.

Photoswitching experiments. Photo-irradiation of liquid samples was carried out using Thorlabs high-power mounted LEDs (models M625 L4 (red, 625 nm, 920 mW); M590 L4 (Amber, 590 nm, 300 mW). Half-lives were determined by UV-Vis spectroscopy by irradiating the sample inside the spectrometer and following a single wavelength for the compound over time. Data was fitted using Origin Pro using an exponential decay model to determine the half-life.

Vesicle preparation. A thin film of lipid (1-palmitoyl-2-oleoyl-sn-3-phosphatidylcholine POPC, egg-yolk phosphatidylglycerol EYPG or

dipalmitoyl phosphatidylcholine DPPC) was formed by evaporating a chloroform solution under a stream of nitrogen gas, and then under high vacuum for 6 h. The lipid film was hydrated by vortexing with the prepared buffer (100 mM NaCl, 10 mM HEPES, 1 mM 8-hydroxypyrene-1,3,6-trisulfonic acid trisodium salt (HPTS), pH 7.0). The lipid suspension was then subjected to 5 freeze-thaw cycles using liquid nitrogen and a water bath (40 °C), followed by extrusion 19 times through a polycarbonate membrane (pore size 200 nm) at rt. Extrusion was performed at 50 °C in the case of DPPC lipids. Extra-vesicular components were removed by size exclusion chromatography on a Sephadex G-25 column with 100 mM NaCl, 10 mM HEPES, pH 7.0. Final conditions: LUVs (2.5 mM lipid); inside 100 mM NaCl, 10 mM HEPES, 1 mM HPTS, pH 7.0; outside: 100 mM NaCl, 10 mM HEPES, pH 7.0.

Transport assays with HPTS. In a typical experiment, the LUVs containing HPTS (25 μL, final lipid concentration 31 μM) were added to buffer (1950 μL of 100 mM NaCl, 10 mM HEPES, pH 7.0) at 25 °C under gentle stirring. A pulse of NaOH (20 μL, 0.5 M) was added at 20 secs to initiate the experiment. At 80 s the test transporter (various concentrations, in 5 μL DMSO) was added, followed by detergent (25 μL of Triton X-100 in 7:1 (v/v) H_2O-DMSO) at 300 secs to calibrate the assay. The fluorescence emission was monitored at $\lambda_{em} = 510$ nm ($\lambda_{ex} = 460/405$ nm).

In-situ transport assays with HPTS (S_4-Sq). LUVs containing HPTS (25 μL, final lipid concentration 31 μM) were added to buffer (1950 μL of 100 mM NaCl, 10 mM HEPES, pH 7.0) at 25 °C under gentle stirring. A pulse of NaOH (20 μL, 0.5 M) was added at 20 secs to initiate the experiment. At 80 s, **S_4-sq** (in 5 μL DMSO) was added. The experiment was recorded using a 510 nm bandpass filter FBH510-10 (Transmission: > 90% AT 510 nm, FWHM: 10 nm. Blocking: > OD5 200–497 nm AND 523–1200 nm)–this enables detection of the HPTS emission at 510 nm, but filters the tailing wavelengths of the Thorlabs M590 L4 LED). The LED was mounted with a focusing lens and placed into the injection chamber of the spectrometer. The lamp was switched on at t = 120 s, and switched off at t = 320 seconds.

In-situ transport assays with HPTS (I_4-Sq). In a fluorescence cuvette, the LUVs containing HPTS (40 μL, final lipid concentration 31 μM) were added to buffer (2890 μL of 100 mM NaCl, 10 mM HEPES, pH 7.0) at 25 °C under gentle stirring. **I_4-sq** (final concentration 66 nM) was added as a DMSO solution to the cuvette. A pulse of NaOH (30 μL, 0.5 M) was added at 50 secs to create the pH gradient across the lipid membrane to initiate the experiment. Finally, detergent (40 μL of Triton X-100 in 7:1 (v/v) H_2O-DMSO) was added at 200 secs to calibrate the assay. The fluorescence emission was monitored at $\lambda_{em} = 510$ nm ($\lambda_{ex} = 460/405$ nm).

Acknowledgements

A. K. acknowledges the EPSRC Centre for Doctoral Training in Synthesis for Biology and Medicine for a studentship (EP/L015838/1), generously supported by AstraZeneca, Diamond Light Source, Defence Science and Technology Laboratory, Evotec, GlaxoSmithKline, Janssen, Novartis, Pfizer, Syngenta, Takeda, UCB and Vertex. M.A. and M.J.L. acknowledge the Leverhulme Trust (RPG-2020-130) for financial support. M.J.L. is a Royal Society University Research Fellow.

Conflict of Interests

The authors declare no conflict of interest.

Data Availability Statement

The data that support the findings of this study are available in the supplementary material of this article.

Keywords: Anion transport · Molecular photoswitch · Azobenzene · Membranes · Anions

[1] D. C. Gadsby, *Nat. Rev. Mol. Cell Biol.* **2009**, *10*, 344–352.
[2] N. J. Yang, M. J. Hinner, *Methods Mol. Biol.* **2015**, *1266*, 29–53.
[3] J. T. Davis, P. A. Gale, R. Quesada, *Chem. Soc. Rev.* **2020**, *49*, 6056–6086.
[4] L. E. Bickerton, T. G. Johnson, A. Kerckhoffs, M. J. Langton, *Chem. Sci.* **2021**, *12*, 11252–11274.
[5] A. Roy, P. Talukdar, *ChemBioChem* **2021**, *22*, 2925–2940.
[6] H. Li, H. Valkenier, A. G. Thorne, C. M. Dias, J. A. Cooper, M. Kieffer, N. Busschaert, P. A. Gale, D. N. Sheppard, A. P. Davis, *Chem. Sci.* **2019**, *10*, 9663–9672.
[7] N. Busschaert, S. H. Park, K. H. Baek, Y. P. Choi, J. Park, E. N. W. Howe, J. R. Hiscock, L. E. Karagiannidis, I. Marques, V. Félix, W. Namkung, J. L. Sessler, P. A. Gale, I. Shin, *Nat. Chem.* **2017**, *9*, 667–675.
[8] J. B. Kim, *Korean J. Pediatr.* **2014**, *57*, 1–18.
[9] M. Ahmad, S. A. Gartland, M. J. Langton, *Angew. Chem. Int. Ed.* **2023**, *62*, e202308842.
[10] S. B. Salunke, J. A. Malla, P. Talukdar, *Angew. Chem. Int. Ed.* **2019**, *58*, 5354–5358.
[11] T. G. Johnson, A. Sadeghi-Kelishadi, M. J. Langton, *J. Am. Chem. Soc.* **2022**, *144*, 10455–10461.
[12] S. J. Wezenberg, L.-J. Chen, J. E. Bos, B. L. Feringa, E. N. W. Howe, X. Wu, M. A. Siegler, P. A. Gale, *J. Am. Chem. Soc.* **2022**, *144*, 331–338.
[13] L. E. Bickerton, M. J. Langton, *Chem. Sci.* **2022**, *13*, 9531–9536.
[14] X. Wu, J. R. Small, A. Cataldo, A. M. Withecombe, P. Turner, P. A. Gale, *Angew. Chem. Int. Ed.* **2019**, *58*, 15142–15147.
[15] Y. R. Choi, B. Lee, J. Park, W. Namkung, K.-S. Jeong, *J. Am. Chem. Soc.* **2016**, *138*, 15319–15322.
[16] M. Ahmad, T. G. Johnson, M. Flerin, F. Duarte, M. J. Langton, *Angew. Chem. Int. Ed.* **2024**, *63*, e202403314
[17] A. Docker, T. G. Johnson, H. Kuhn, Z. Zhang, M. J. Langton, *J. Am. Chem. Soc.* **2023**, *145*, 2661–2668.
[18] B. Zhou, F. P. Gabbaï, *Chem. Sci.* **2020**, *11*, 7495–7500.
[19] M. M. Lerch, M. J. Hansen, W. A. Velema, W. Szymanski, B. L. Feringa, *Nat. Commun.* **2016**, *7*, 12054.
[20] P. Kobauri, F. J. Dekker, W. Szymanski, B. L. Feringa, *Angew. Chem. Int. Ed.* **2023**, *62*, e202300681.
[21] M. J. Fuchter, *J. Med. Chem.* **2020**, *63*, 11436–11447.
[22] W. A. Velema, W. Szymanski, B. L. Feringa, *J. Am. Chem. Soc.* **2014**, *136*, 2178–2191.
[23] D. B. Konrad, G. Savasci, L. Allmendinger, D. Trauner, C. Ochsenfeld, A. M. Ali, *J. Am. Chem. Soc.* **2020**, *142*, 6538–6547.
[24] G. Testolin, J. Richter, A. Ritter, H. Prochnow, J. Köhnke, M. Brönstrup, *Chem. – Eur. J.* **2022**, *28*, e202201297.
[25] M. Wegener, M. J. Hansen, A. J. M. Driessen, W. Szymanski, B. L. Feringa, *J. Am. Chem. Soc.* **2017**, *139*, 17979–17986.
[26] M. Volgraf, P. Gorostiza, S. Szobota, M. R. Helix, E. Y. Isacoff, D. Trauner, *J. Am. Chem. Soc.* **2007**, *129*, 260–261.
[27] K. Hüll, J. Morstein, D. Trauner, *Chem. Rev.* **2018**, *118*, 10710–10747.
[28] V. A. Gutzeit, A. Acosta-Ruiz, H. Munguba, S. Häfner, A. Landra-Willm, B. Mathes, J. Mony, D. Yarotski, K. Börjesson, C. Liston, G. Sandoz, J. Levitz, J. Broichhagen, *Cell Chem. Biol.* **2021**, *28*, 1648–1663.e1616.
[29] M. Ahmad, S. Metya, A. Das, P. Talukdar, *Chem. – Eur. J.* **2020**, *26*, 8703–8708.
[30] J. A. Peterson, C. Wijesooriya, E. J. Gehrmann, K. M. Mahoney, P. P. Goswami, T. R. Albright, A. Syed, A. S. Dutton, E. A. Smith, A. H. Winter, *J. Am. Chem. Soc.* **2018**, *140*, 7343–7346.
[31] M. Dong, A. Babalhavaeji, S. Samanta, A. A. Beharry, G. A. Woolley, *Acc. Chem. Res.* **2015**, *48*, 2662–2670.

[32] C. Knie, M. Utecht, F. Zhao, H. Kulla, S. Kovalenko, A. M. Brouwer, P. Saalfrank, S. Hecht, D. Bléger, *Chem. – Eur. J.* **2014**, *20*, 16492–16501.
[33] A. Kerckhoffs, Z. Bo, S. E. Penty, F. Duarte, M. J. Langton, *Org. Biomol. Chem.* **2021**, *19*, 9058–9067.
[34] A. Kerckhoffs, M. J. Langton, *Chem. Sci.* **2020**, *11*, 6325–6331.
[35] J. Volarić, W. Szymanski, N. A. Simeth, B. L. Feringa, *Chem. Soc. Rev.* **2021**, *50*, 12377–12449.
[36] M. Dong, A. Babalhavaeji, C. V. Collins, K. Jarrah, O. Sadovski, Q. Dai, G. A. Woolley, *J. Am. Chem. Soc.* **2017**, *139*, 13483–13486.
[37] S. Samanta, T. M. McCormick, S. K. Schmidt, D. S. Seferos, G. A. Woolley, *Chem. Commun.* **2013**, *49*, 10314–10316.
[38] D. Bléger, J. Schwarz, A. M. Brouwer, S. Hecht, *J. Am. Chem. Soc.* **2012**, *134*, 20597–20600.
[39] A. Kerckhoffs, K. E. Christensen, M. J. Langton, *Chem. Sci.* **2022**, *13*, 11551–11559.
[40] S. J. Edwards, I. Marques, C. M. Dias, R. A. Tromans, N. R. Lees, V. Félix, H. Valkenier, A. P. Davis, *Chem. – Eur. J.* **2016**, *22*, 2004–2011.
[41] H. Valkenier, C. J. E. Haynes, J. Herniman, P. A. Gale, A. P. Davis, *Chem. Sci.* **2014**, *5*, 1128–1134.
[42] A. Kerckhoffs, I. Moss, M. J. Langton, *Chem. Commun.* **2023**, *59*, 51–54.
[43] I. V. Tetko, J. Gasteiger, R. Todeschini, A. Mauri, D. Livingstone, P. Ertl, V. A. Palyulin, E. V. Radchenko, N. S. Zefirov, A. S. Makarenko, V. Y. Tanchuk, V. V. Prokopenko, *J. Comput. Aided Mol. Des.* **2005**, *19*, 453–463.
[44] V. Saggiomo, S. Otto, I. Marques, V. Félix, T. Torroba, R. Quesada, *Chem. Commun.* **2012**, *48*, 5274–5276.
[45] M. J. Spooner, P. A. Gale, *Chem. Commun.* **2015**, *51*, 4883–4886.

Manuscript received: June 21, 2024
Accepted manuscript online: August 1, 2024
Version of record online: October 29, 2024